Ag_2O band structure and x-ray-absorption near-edge spectra

M. T. Czyżyk and R. A. de Groot
Faculteit der Wiskunde en Natuurwetenschappen, Katholieke Universiteit Nijmegen, Toernooiveld, NL-6525 ED Nijmegen, The Netherlands

G. Dalba, P. Fornasini, and A. Kisiel*
Dipartimento di Fisica, Università degli Studi di Trento, I-38050 Povo (Trento), Italy

F. Rocca
Centro di Fisica degli Stati Aggregati e Impianto Ionico del Consiglio Nazionale delle Ricerche, I-38050 Povo (Trento), Italy

E. Burattini
Laboratoire Nazionali di Frascati, Istituto Nazionale di Fisica Nucleare, Cassella Postale 13, I-00044 Frascati (Roma), Italy
(Received 22 December 1988)

The x-ray-absorption spectra of Ag_2O are reported. Good agreement is obtained with a band-structure calculation using the atomic-sphere approximation with an extended basis set. The observation of the white line is an indication of the nonclosed 4*d* shell of Ag in this compound, although the exciton contribution cannot be ruled out.

I. INTRODUCTION

The interest in the study of unoccupied electronic states in solids is steadily growing. On the experimental side, techniques like x-ray-absorption spectroscopy (XAS), which for solids is commonly divided into x-ray-absorption near-edge spectroscopy[1–4] (XANES) and extended x-ray-absorption fine structure (EXAFS),[5–7] and the relatively new bremsstrahlung isochromat spectroscopy[8–10] (BIS) are commonly employed. XAS consists of measuring the fine structures of the x-ray-absorption coefficient at and above the absorption edges. In the vicinity of an absorption edge, while the energy dependence of the transition-matrix element is in general slow, the XAS structures directly reflect the shape of the partial density of states of the unoccupied bands projected on the atom under study.

Also, much theoretical work, both within a one-particle and a many-body framework was done in order to reproduce and interpret the experimental results. The question to what extent the one-particle band approach is adequate is still open and its investigation is hampered by calculational difficulties. There is some evidence in the literature that many-body effects (Nozières–de Dominicis[11–13] enhancement) are smaller than previously believed, at least for metals.[14,1–3] On the other hand, the energy ranges of the calculated x-ray-absorption spectra (with the exception of the work of Muller *et al.*[2,3]) were usually limited to few eV above the absorption threshold. Moreover, the calculations were performed for simple systems only (mostly with one atom in the unit cell). This seems to indicate the technical difficulties in obtaining description of bands accurate enough for energies higher than, say, 10 eV above the Fermi level for the more complex systems.

The validity of one-particle band approach for the description of the x-ray absorption in insulators and semiconductors appears, in general, more questionable. It is expected that for these materials, excitonic effects (the core-hole–electron interaction) can modify the results obtained through band-structure ground-state calculation to a greater extent than in the case of metals, and different opinions concerning this problem are presented in the literature.[15–17]

The purpose of this paper is twofold. The first aim is both an experimental and theoretical systematic study of the electronic structure of Ag_2O. This compound has a highly symmetrical cubic structure: silver atoms are linearly coordinated by oxygens and oxygen atoms are tetrahedraly coordinated by silver atoms.[18] The low coordination of the metal atom with oxygen is rather unusual (the only other compound with this structure being the isoelectronic Cu_2O). On the basis of molecular-orbital considerations, this was attributed to a relatively small energy difference between the filled 4*d* and the unfilled 5*s* orbitals of silver, which favors the hybridization of the d_{z^2} and *s* orbitals.[19]

The knowledge of the electronic structure of Ag_2O is still incomplete and a better understanding of it is highly desirable.

(a) Ag_2O has the same crystal structure as Cu_2O which is presently widely studied in view of the role of copper oxides in high-T_c superconducting compounds.

(b) Ag_2O is utilized as a modifier oxide in fast ion conducting glasses of the type AgI-Ag_2O-B_2O_3. A detailed knowledge of the electronic structure of crystalline Ag_2O will help to understand the characteristics of the chemical bonds between Ag and O in the glasses. This in turn should facilitate the understanding of the local structure of the glass and the still controversial mechanism of ionic conduction.[20,21]

The second aim is to contribute to the discussion on the applicability of the one-particle band approach for the description of the x-ray near-edge spectra in semiconductors.

For these purposes, we investigated the electronic structure of Ag_2O by XAS measurements at the L_1, L_2, and L_3 edges of silver and by carrying out the band-structure calculation by the augmented–localized-spherical wave (ALSW) method with an extended basis set.

This paper is organized as follows. In Sec. II the most important details concerning the experimental apparatus and measurements are summarized and the experimental results are reported. In Sec. III the results of the band-structure calculation are presented including partial densities of states, and partial charges, and the structure of the valence bands is addressed. In Sec. IV the calculation of x-ray Ag L_1, L_2, and L_3 spectra is described and the experimental and theoretical results are compared. Section V contains a discussion and conclusions.

II. EXPERIMENTAL DETAILS AND RESULTS

The x-ray-absorption measurements at the L edges of silver have been performed in the transmission mode with synchrotron radiation (SR) at the wiggler source in Frascati.[22] In order to obtain a homogeneous sample of uniform thickness as required by the XAS technique, we deposited the required amount of Ag_2O powder on filter paper utilizing an ultrasonic mixer. The x-ray beam was monochromatized by a silicon channel-cut crystal with reflecting faces (111). All measurements were performed at room temperature. The three edges, L_1, L_2 and L_3 have been measured on the same sample in the same experimental conditions; the edges L_2 and L_3 have been measured in the same acquisition run.

The energy resolution of the experimental apparatus is determined by (a) the finite width ΔE_m of the rocking curve of the crystal monochromator and (b) the finite angular divergence ΔE_b of the SR beam in the vertical plane as determined by the collimating slits. For all three L edges of silver (L_1, L_2, and L_3) we estimated $\Delta E_m = 0.5$ eV and $\Delta E_b = 0.4$ eV. From the quadratic sum of ΔE_m and ΔE_b, the overall FWHM instrumental Gaussian broadening $\Gamma_g = 0.64$ eV was found.

The spectra were originally measured to analyze the EXAFS at the edges L_3 and L_1 and the experimental setup was optimized accordingly.[23] Therefore the experimental points were recorded with a spacing of 0.25 eV at the edges L_2 and L_3 and 0.4 eV at the edge L_1. This is quite satisfactory because the experimental Gaussian broadening Γ_g is reasonably smaller than the Lorentzian broadening due to the finite lifetime of the excited core states. The values of the core-level widths of silver quoted in the review paper by Sevier[24] are 5.3–6.5 eV for the L_1 edge and 2.06–2.42 and 1.8–2.3 eV for the edges L_2 and L_3, respectively (see also Ref. 25).

During the data reduction, the contribution of each edge to the absorption coefficient was isolated by a Victoreen-like extrapolation of the preedge region to the higher energies.

In Fig. 1, we present the Ag L_1, L_2, and L_3 edges of polycrystalline Ag_2O obtained by this procedure compared with the corresponding edges of a metallic silver in the form of a thin foil. The energy scales are relative to the absorption threshold E_0 of each edge, conventionally chosen at the maximum of the first derivative.

III. BAND-STRUCTURE CALCULATION

Band-structure calculations were performed by the ALSW method with the extended basis set. In this method, the idea of the most localized muffin-tin orbitals of Andersen and Jepsen[26] and Andersen *et al.*[27] was adopted for the augmented-spherical-wave (ASW) method of Williams *et al.*[28] The ASW and linear muffin-

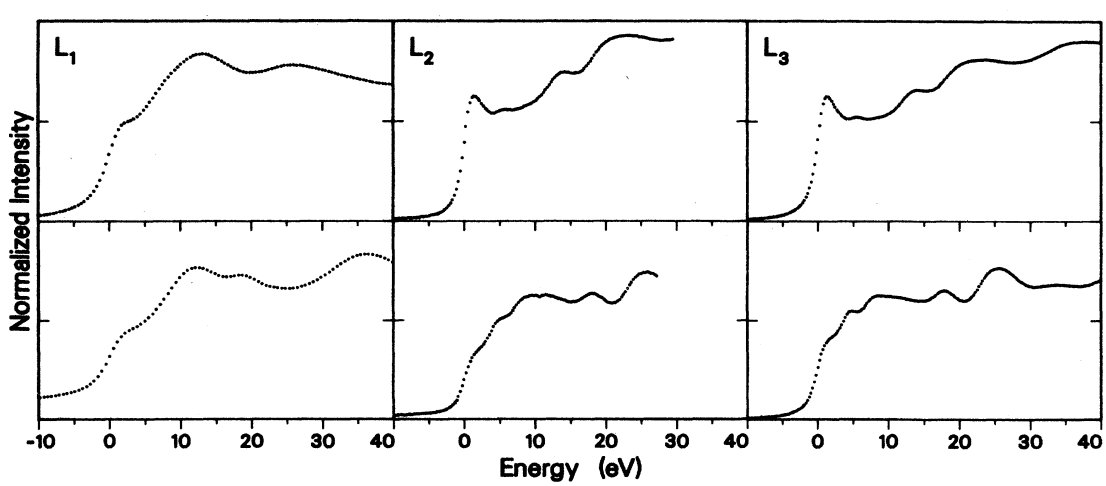

FIG. 1. L absorption edges of Ag_2O (top) and metallic silver (bottom) in the arbitrary units.

tin orbital (LMTO) methods have been extremely useful in the calculation of occupied states. The disadvantage of the methods is that they cannot describe higher unoccupied states. This is because the basis set includes one spherical wave (SW) only for each quantum number l and atomic site only. Each SW is augmented inside the atomic spheres by the solution of the radial Schrödinger equation with the number of nodes appropriate for the optimal description of the valence bands. A proper description of higher unoccupied states requires more basis functions than needed for the description of the occupied states alone. Therefore, we extend the basis set by adding more SW per l and atomic site with an increasing number of nodes in the augmenting function.[29] Such a procedure possesses the advantages of the use of different energy parameters in energy panels in the linear augmented–plane-wave (LAPW), LMTO, and ASW methods, but without the obvious disadvantages created by that process. The price to be paid is the increased size of the secular matrix. This is not prohibitive, however, because the self-consistent field (SCF) run itself does not need the extended states, they are added in some last iterations and in the calculation of observables. The main time is still spent in the SCF cycle. The method was reimplemented for the vector processing on supercomputers (for more details see Ref. 30).

We used the scalar-relativistic Hamiltonian [spin-orbit (s.o) interaction not included] and the exchange and correlation effects were treated by the local density approximation using the Hedin and Lundqvist[31] parametrization. The self-consistent calculation was carried out including all core electrons.

Ag_2O crystallizes in the simple-cubic structure, which belongs to the space group $Pn3m$ (O_{4h}^3). There are four Ag and two O atoms in the unit cell at 4b [$(\frac{1}{4},\frac{1}{4},\frac{1}{4})$] and 2a [(0,0,0)] Wyckoff positions, respectively. This constitutes a very loosely packed structure and therefore in order to fill the unit cell as much as possible with atomic spheres, we located "empty" atomic spheres at the complementary Wyckoff positions 4c [$(\frac{3}{4},\frac{3}{4},\frac{3}{4})$] and 6d [$(0,\frac{1}{2},\frac{1}{2})$]. The radii of the atomic spheres in the order given above are 2.424, 1.906, 2.424, and 1.906 a.u.

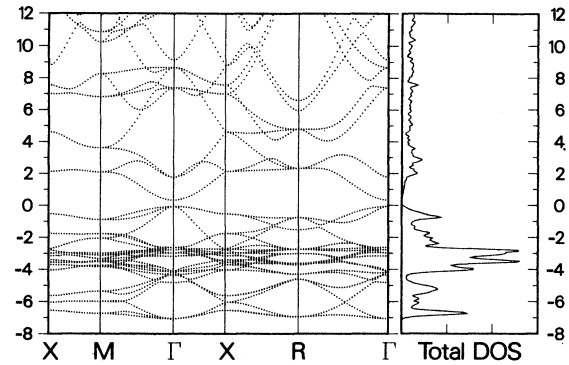

FIG. 2. Band structure and total density of states of Ag_2O. The energy zero is shifted to the top of the valence band. The band originating mainly from O 2s is lying between -18.76 and -18.17 eV and it is not shown. DOS is given in number of states of spins per eV unit cell.

The self-consistent iteration was performed with 35 **k** points uniformly distributed in an irreducible part of the first Brillouin zone (IBZ) (512 in the whole BZ) until the changes of the local partial charges in each atomic sphere were smaller than 10^{-6} electrons. At the same time the changes of the eigenvalues were generally smaller than 0.1 mRy. Next, the histograms of the partial density of states were constructed by solving the Hamiltonian in

TABLE I. Energy eigenvalues at the symmetry points Γ, X, M, R in rydbergs. Irreducible representations (IR) are also indicated. The constant potential $V_0=-0.6673$ Ry and the top of the valence bands (Γ'_{25}) is at -0.0836 Ry.

IR	Γ	IR	X	IR	M	IR	R
1	−1.4628	1	−1.4419	1	−1.4417	1	−1.4664
2′	−1.4191	4	−0.5591	3	−0.5737	2′	−1.4149
25′	−0.5970	1	−0.5220	1	−0.5185	25′	−0.5887
1	−0.4326	3	−0.4922	4	−0.4720	15	−0.4177
12	−0.3872	1	−0.3752	3	−0.3597	25′	−0.3955
15	−0.3830	2	−0.3508	1	−0.3541	12	−0.3523
25′	−0.3826	1	−0.3388	3	−0.3374	15′	−0.3447
12	−0.3117	3	−0.3282	4	−0.3316	25′	−0.3009
25′	−0.2970	4	−0.3099	2	−0.3237	15′	−0.2805
15′	−0.2825	2	−0.2974	2	−0.3073	12	−0.2804
15′	−0.2715	1	−0.2808	1	−0.2983	1	−0.1909
25′	−0.0836	4	−0.2793	3	−0.2293	25′	−0.1349
1	−0.0539	3	−0.2074	4	−0.2083	15	0.0915
12′	0.0526	4	−0.1169	1	−0.1437	25′	0.2732
25′	0.4649	1	0.0782	1	0.0750	2′	0.3583
25	0.5583	2	0.2610	3	0.1870	1	0.4058
2′	0.5937	3	0.4364	3	0.4225		
		4	0.4782	4	0.5298		
		1	0.5685				

TABLE II. Partial charges in electrons per atom at given site.

Site	$l=0$	$l=1$	$l=2$	$l=3$	Total
Ag	0.3295	0.1920	8.9521	0.0402	9.5138
O	1.7359	4.2321	0.0695		6.0375
Empty sphere 1	0.3056	0.3230	0.1559		0.7845
Empty sphere 2	0.2498	0.1475	0.0580		0.4553

165 **k** points in IBZ (4096 in the whole BZ).

The conventional basis we used in the SCF run contained the SW's augmented in atomic spheres by the solutions of Schrödinger equation with l value and the number of nodes indicated by atomiclike symbols: $5s$, $5p$, $4d$, and $4f$ at the Ag site; $2s$, $2p$, and $3d$ at the O site; and $1s$, $2p$, and $3d$ at each "empty" atomic sphere. After the self-consistency was achieved, the basis set was extended by the SW augmented by $5d$-like function at the Ag site and then the self-consistency was reachieved. The differences of eigenvalues resulting from these two calculations are smaller than 1 mRy as far as the valence bands are concerned. However, they become important already a few eV above the bottom of the conduction band.

The band structure obtained with the extended basis set together with the total density of states is presented in Fig. 2. The eigenvalues at selected symmetry points are listed in Table I.

It is not a purpose of this article to deeply discuss the structure of the valence states and the binding mechanism of Ag_2O, nevertheless we will stress the most important features of that structure. As one can see from Figs. 3 and 4, where the partial density of the valence states at the Ag and O sites are shown, as well as from Table II, which gives the partial charges, the valence bands are basically built out of Ag $4d$ and O $2p$ states. The contributions from other states are at least one order of magnitude smaller. The bottom of the valence band has mostly O p character. Next, a group of flat Ag $4d$ bands is located between -4.5 and -2.5 eV and the highest part of the valence band consists of O p and Ag d hybridized states. There is also a small but important contribution of Ag $5s$-originating states throughout the valence bands.

In general, the structure of the valence bands and the

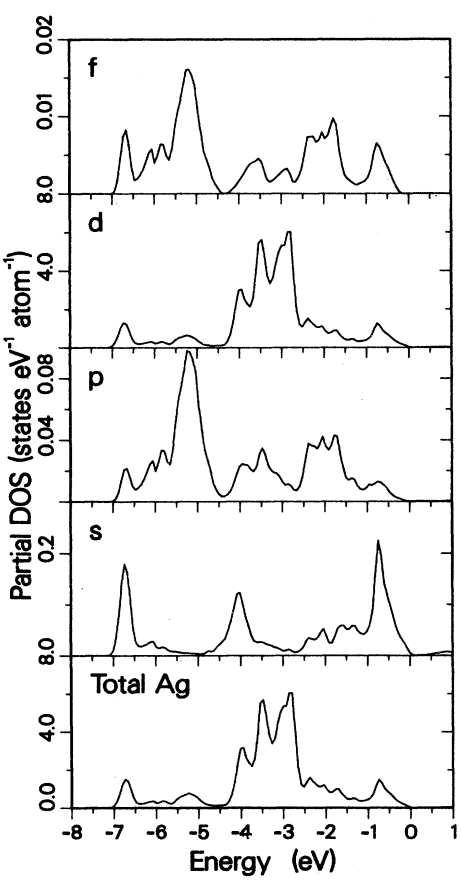

FIG. 3. Partial density of valence states at the Ag site.

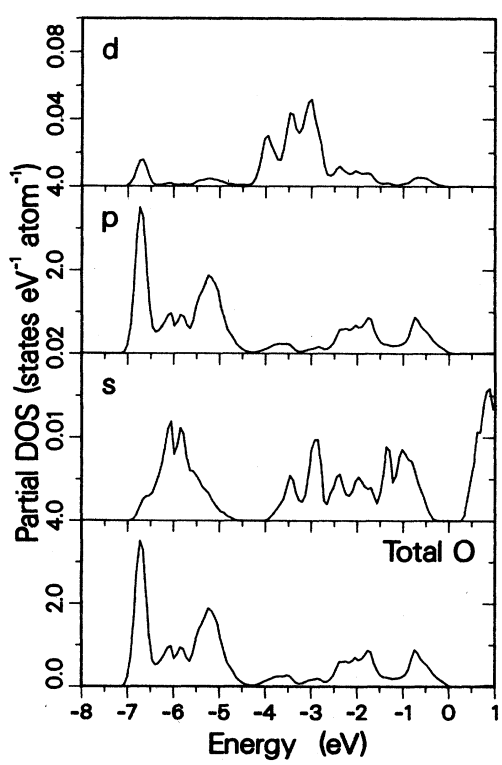

FIG. 4. Partial density of valence states at the O site.

binding mechanism of Ag_2O are quite the same as those in Cu_2O described in detail by Marksteiner *et al.*[32] The same conclusions about Cu_2O were reobtained as a part of a wider study of copper oxides properties to be discussed elsewhere.[30]

IV. CALCULATION OF X-RAY-ABSORPTION SPECTRA

The main aim of our theoretical work is to obtain the x-ray-absorption spectra from first-principles band-structure calculations in a relatively large range of energies. According to the simple atomic-based selection rules, the edge L_1 is due to transitions from $2s$ to p-like unoccupied states and the edges $L_{2,3}$ to transitions from $2p$ to s- and d-like states. Within the constant-matrix-element approximation the theoretical spectra were obtained by the convolution of the relevant partial density of unoccupied states, presented in Fig. 5, with the Lorentzian and Gaussian energy distributions which account for the core-level and final-state lifetime and the instrumental effects, respectively. The values of the Gaussian full width at half maximum (FWHM) parameter used was 0.64 eV as estimated from experiment, but the FWHM of the Lorentzian distribution was optimized to obtain the best agreement of the theoretical spectra with the measured ones in the vicinity (10 eV around) of the absorption edges. Additionally, the energy dependent term of the form 0.1 $(E-E_0)$ was added to the Lorentzian FWHM to account for the increase of the final-state lifetime. The relevant parameters for the construction of the x-ray spectra are summarized in Table III.

The results for Ag L_1 and L_3 edges obtained by calculation with the conventional basis set are compared with experiment in Fig. 6. The poor agreement in the case of the L_3 edge already a few eV above the absorption edge is apparent. As we stressed above (see Table II) Ag has a nearly filled $4d$ shell and the d-like functions at the Ag site consequently contribute little to the DOS in the conduction band. On the contrary, the agreement in the case of the L_1 edge is reasonably good because the p-like $(l=1)$ functions at the Ag site have their spectral weight above the gap (see Table II) and work effectively in an higher-energy range. The analysis given above clearly shows why it is necessary to go beyond the conventional basis set and why we extended this set just by the SW augmented by $5d$-like functions at the Ag site.

Figure 7 presents the Ag L_1, L_2, and L_3 edges obtained with the extended basis set. The essential improvement of the description of the L_3 spectrum is evident, and the same was found for the L_2 spectrum. As a second-order effect an improvement in the calculated L_1 spectrum is observed. This is because the introduction of the $5d$ function modifies the interaction of the $5p$ func-

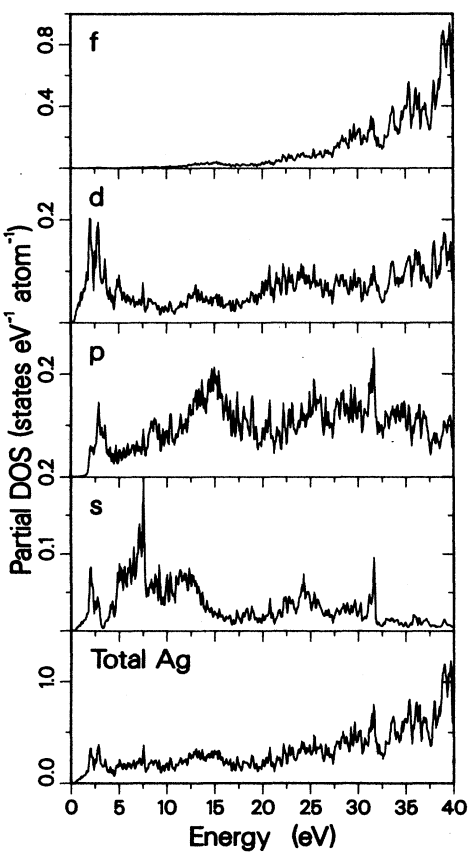

FIG. 5. Partial density of unoccupied states at the Ag site.

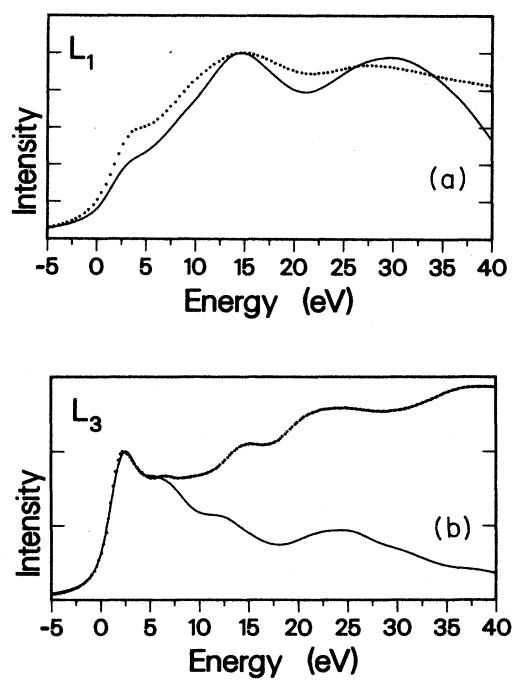

FIG. 6. Comparison between x-ray-absorption spectra (a) Ag L_1 and (b) Ag L_3 obtained by calculation with the conventional basis set and the measured ones. The normalization of theoretical curves to experimental spectra has been done at the first peak and then the derivatives were calculated.

TABLE III. Lorentzian and Gaussian broadening parameters in eV as used for the calculation of the x-ray spectra. The ratio between d and s DOS for L_2 and L_3 edges was treated as an adjustable parameter because we do not calculate the transition-matrix elements.

Spectrum	Contributing density of states at Ag site	Lorentzian FWHM	Gaussian FWHM
Ag L_1	p DOS	$4.0+0.1(E-E_0)$	0.64
Ag L_2	d DOS+0.5(s DOS)	$2.1+0.1(E-E_0)$	0.64
Ag L_3	d DOS+0.5(s DOS)	$1.9+0.1(E-E_0)$	0.64

tions with neighboring atoms substantially and hence has an important indirect influence on the L_1 spectrum as well. By the same line of reasoning it is a valid question to ask whether an extension of the basis set with oxygen $3s,p$ functions could have an influence on the Ag L_1 and $L_{2,3}$ spectra. The influence of these functions, however, was found to take place at energies higher than the ones we are interested in here.

V. DISCUSSION AND CONCLUSIONS

First, we would like to consider in some details the comparison between the edges L_2 and L_3. These edges

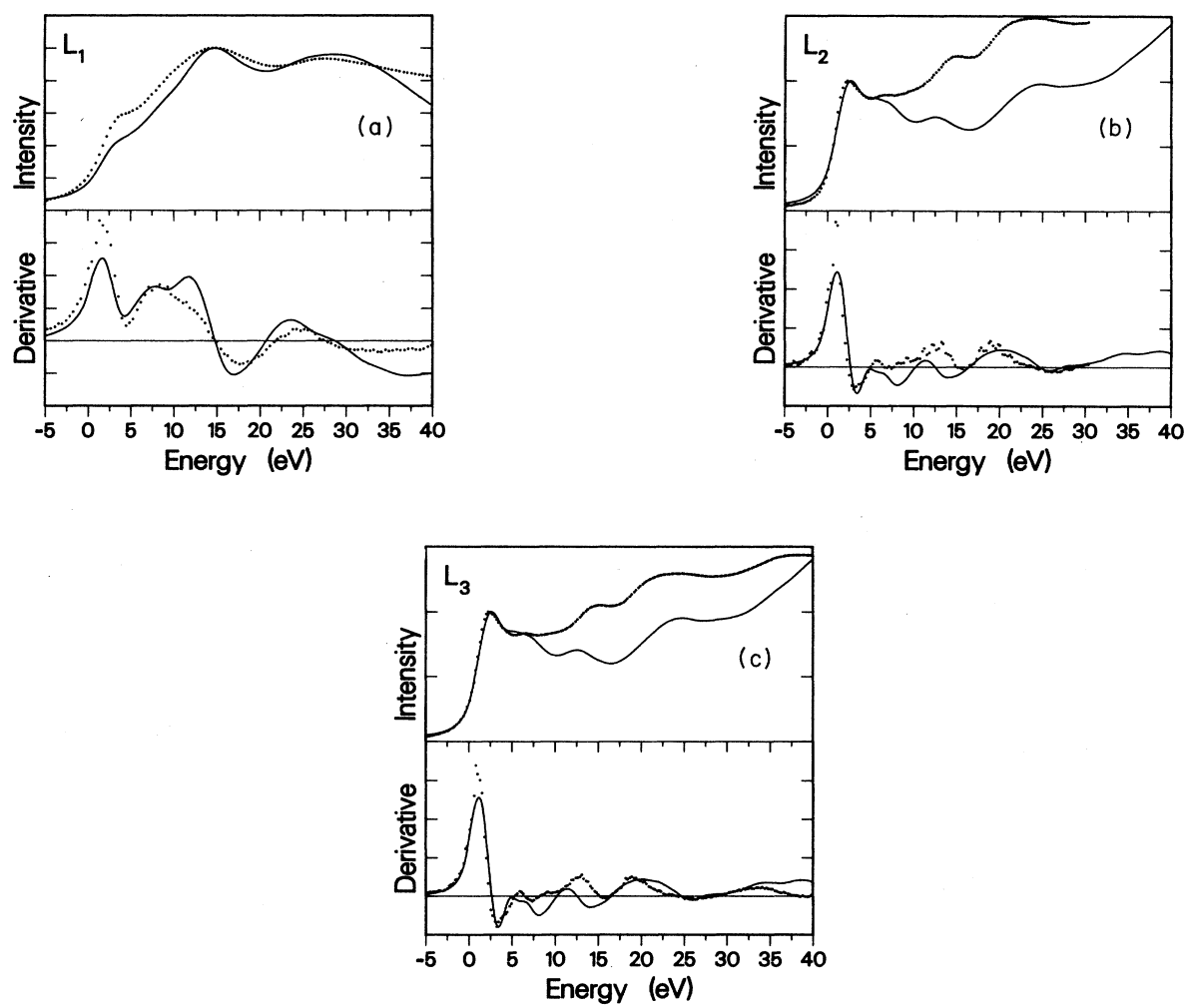

FIG. 7. Comparison between x-ray-absorption spectra (a) Ag L_1, (b) Ag L_2, and (c) Ag L_3, obtained by calculations with the extended basis set and the measured ones. The normalization of theoretical curves to experimental spectra has been done at the first peak and then the derivatives were calculated.

are due to transitions from $2p$ levels with $j=\frac{1}{2}$ and $j=\frac{3}{2}$, respectively. The statistical ratio 2:1 of the populations of the core levels $2p_{3/2}$ and $2p_{1/2}$ is reflected in the expected ratio 2:1 between the mean absorption coefficients of the two edges. The possible deviations from the expected ratio 2:1 are due to the final-state effects. For the final state with the d shell almost completely filled, as in the case of Ag, the differences between the L_2 and L_3 near-edge structures can monitor the j character of the unoccupied states above the Fermi level (while $j=\frac{3}{2}$ is allowed in both L_2 and L_3, $j=\frac{5}{2}$ is forbidden in L_2). In Fig. 8 the measured Ag L_3 and L_2 edges of Ag_2O are compared. Spectra have been normalized in the region beyond 20 eV. The difference between the two spectra of Ag_2O in the region 0–10 eV is clearly seen. These kinds of differences have been satisfactorily explained in similar cases by Brown *et al.*[33] and by Benfatto *et al.*[34] in terms of prevailing $d_{5/2}$ states immediately above the Fermi level, considering negligible the contribution of many-body effects. In our calculations, we have used the scalar-relativistic Hamiltonian (i.e., spin-orbit coupling is neglected) and therefore we cannot resolve that problem here.

Secondly, we would like to attract the reader's attention once again to Fig. 5 which presents the unoccupied states at the Ag site. Although, the Ag $4d$ shell is filled for about 90% (as pointed out already above, see Table II) the unoccupied silver $4d$ states are also present at the very bottom of the conduction band (up to ≈ 4 eV). Just these d states contribute the most to the leading peak at the L_3 and L_2 absorption edges. The same was found for the Cu L_3 and L_2 edges in Cu_2O.[30] (The similarity of the electronic structure of these two compounds was already stressed above.)

We do expect that the core-hole–electron interaction (in other words, the core exciton) may even substantially narrow the linewidth and/or increase the slope of the absorption edge (see the discussion below), but we are convinced that the leading peak (white line) at the metal L_3 and L_2 x-ray-absorption edges in Ag_2O (and in Cu_2O) is mainly due to the sharp d-like density of states just above the bottom of conduction band. This result is in some contradiction with the paper of Hulbert *et al.*[35] where the entire effect was ascribed to the core exiton.

Finally, we would like to contribute to the discussion about the applicability of the one-particle approach to the description of the x-ray absorption in the semiconductors. As one can see from Fig. 7, for all three Ag edges L_1, L_2, and L_3 we have obtained good agreement between the theory and experiment. The conclusion from this work is that the ground-state band-structure calculation is able to quantitatively explain the x-ray near-edge spectra of Ag_2O.[36] In order to obtain better results in the higher-energy range, however, the use of the ALSW (or LMTO) method for calculation of unoccupied states requires extension of the basis set beyond the conventional set as described in Sec. III. We also expect that the inclusion of the transition matrix elements will further improve that agreement in the region of 10–35 eV. In spite of the overall good agreement there is, however, systematic discrepancy in the slope of all three absorption edges, which we clearly present by including the first derivative of the theoretical and experimental spectra in Fig. 7. These discrepancies cannot be reduced either by further adjustments of the broadening parameters without essentially spoiling the agreement in other energy regions, or by the inclusion of the transition-matrix elements which are in general slowly varying with the energy. These discrepancies we ascribe to the many-body effects. In this case they are dominated, in our opinion, by the influence of the core-hole potential. To investigate this problem quantitatively, the fully self-consistent super-cell electronic structure calculations of the final state of the excited system are in progress. Such an approach will take into account the influence of the core hole created during the excitation process as well as the relaxation of the system. We stress, however, that the discrepancies in the slope of absorption edges pointed out above do not unable us in any way to interpret the x-ray near-edge spectra of semiconductors in terms of one-particle theory.

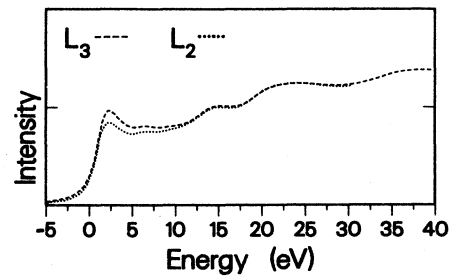

FIG. 8. Comparison between the L_2 and L_3 edges for Ag in Ag_2O. The L_2 and L_3 spectra have been normalized within the 20–30 eV energy interval.

ACKNOWLEDGMENTS

The authors are grateful to the technical staff of the Wiggler Synchrotron Radiation Source in Frascati for their help in XAS measurements. Part of this work was supported by the Stichting voor Fundamenteel Onderzoek der Materie (FOM) with financial support from the Nederlandse Organisatie voor Wetenschappelijk Onderzoek (NWO), The Netherlands.

*On leave from the Institute of Physics, Jagellonian University, Reymonta 4, PL-30-059 Kraków 16, Poland.

[1]J. E. Muller, O. Jepsen, O. K. Andersen, and J. W. Wilkins, Phys. Rev. Lett. **40**, 720 (1978).
[2]J. E. Muller, O. Jepsen, and J. W. Wilkins, Solid State Commun. **42**, 365 (1982).
[3]J. E. Muller and J. W. Wilkins, Phys. Rev. B **29**, 4331 (1984).
[4]G. Dalba, P. Fornsaini, and E. Buratini, J. Phys. C **16**, L1091

(1983).

[5]C. Kunz, in *Synchrotron Radiation, Topics in Current Physics* (Springer, Berlin, 1979), Vol. 10, p. 1.

[6]P. A. Lee, P. H. Citrin, P. Eisenberger, and B. M. Kincaid, Rev. Mod. Phys. **53**, 769 (1981).

[7]*EXAFS and Near Edge Structure III,* Proceedings of the International Conference, Stanford, 1984, edited by K. O. Hodgson, B. Hedman, and J. E. Penner-Hahn (Springer-Verlag, Berlin, 1984).

[8]W. Speier, J. C. Fuggle, R. Zeller, B. Ackermann, K. Szot, F. U. Hillebrecht, and M. Campagna, Phys. Rev. B **30**, 6921 (1984).

[9]W. Speier, R. Zeller, and J. C. Fuggle, Phys. Rev. B **32**, 2597 (1985).

[10]Y. Gao, B. Smandek, T. J. Wagner, J. H. Waever, F. Levy, and G. Margaritondo, Phys. Rev. B **35**, 9357 (1987).

[11]P. Nozières and C. T. De Dominicis, Phys. Rev. **178**, 1097 (1969).

[12]G. D. Mahan, Phys. Rev. **153**, 882 (1967); **163**, 612 (1967).

[13]G. D. Mahan, in *Solid State Physics,* edited by H. Ehrenreich, F. Seitz, and D. Turnbull (Academic, New York, 1974), Vol. 29, p. 75, and references therein.

[14]R. P. Gupta and A. F. Freeman, Phys. Rev. Lett. **36**, 1194 (1976).

[15]B. Poumellec, J. E. Marucco, and B. Tonzelin, Phys. Rev. B **35**, 2284 (1987).

[16]C. Sagiura and S. Maramatsu, Phys. Status Solidi B **129**, K157 (1985).

[17]A. Kisiel, G. Dalba, P. Fornasini, M. Podgórny, J. Oleszkewicz, F. Rocca, and E. Burattini, Phys. Rev. B **39**, 7895 (1989).

[18]W. G. Wyckoff, *Crystal Structures* (Wiley, New York, 1963).

[19]L. E. Orgel, J. Chem. Soc. 4186 (1958).

[20]G. Dalba, P. Fornasini, F. Rocca, and E. Burattini, J. Phys. (Paris) Colloq. **47**, C8-749 (1986).

[21]G. Dalba, P. Fornasini, A. Fontana, F. Rocca, and E. Burattini, Solid State Ionics (to be published).

[22]E. Burattini, E. Bernieri, A. Balerna, C. Mencuccini, R. Rinzivillo, G. Dalba, and P. Fornasini, Nucl. Instrum. Methods A **246**, 125 (1986).

[23]E. Bernieri, E. Burattini, G. Dalba, P. Fornasini, and F. Rocca Solid State Commun. **48**, 421 (1983).

[24]K. D. Sevier, *Low-Energy Electron Spectrometry* (Wiley-Interscience, New York, 1972), p. 230, and references therein.

[25]M. O. Krause and J. H. Oliver, J. Phys. Chem. Ref. Data **8**, 329 (1979).

[26]O. K. Andersen and O. Jepsen, Phys. Rev. Lett. **53**, 2571 (1984).

[27]O. K. Andersen, O. Jepsen, and D. Glötzel, in *Highlights of Condensed Matter Theory,* Proceedings of the International School of Physics "Enrico Fermi," Course LXXXIX, Bologna, 1985, edited by F. Bassani, F. Fumi, and M. Tosi (North-Holland, Amsterdam, 1985), pp. 59–176.

[28]A. R. Williams, J. Kübler, and C. D. Gelatt, Jr., Phys. Rev. B **19**, 6094 (1979).

[29]A related problem is the contribution of states of more than one main quantum number per angular quantum number in states under high compression see e.g., W. Zittel, J. Meyer-ter-Vehn, and J. Kübler, Physica **139&140B**, 364 (1986); Solid State Commun. **62**, 97 (1987). Also, a number of elements in the Periodic Table are not optimally described by traditional LMTO or ASW methods. For, e.g., zinc and gallium it is not possible to treat the 3*d* level as core states, while at the same time there can be a need for the inclusion of the 4*d* valence state. This problem is solved by these approaches.

[30]M. T. Czyżyk and R. A. de Groot (unpublished).

[31]L. Hedin and B. I. Lundqvist, J. Phys. C **3**, 2065 (1971).

[32]P. Marksteiner, P. Blaha, and K. Schwarz, Z. Phys. B **64**, 119 (1986).

[33]M. Brown, R. E. Peierls, and E. A. Stern, Phys. Rev. B **15**, 738 (1977).

[34]M. Benfatto, A. Bianconi, I. Davoli, L. Incoccia, S. Mobilio, and S. Stizza, Solid State Commun. **46**, 367 (1983).

[35]S. L. Hulbert, B. A. Bunker, F. C. Brown, and P. Pianetta, Phys. Rev. B **30**, 2120 (1984).

[36]Similar conclusions from the extended study of cations and anions XANES spectra of ZnTe, CdTe, and HgTe were obtained in Ref. 17.